

# The new Linth-Limmern hydro-power plant – design of caverns under 500 m overburden

R. Marclay, J.-M. Hohberg, M. John, T. Marcher

*Engineering Consortium “Alpenstrom”, Zurich, Switzerland*

*(IM Locarno, IUB Berne, ILF Rum/Austria, ILF Zurich, KBM Sion, R. Andenmatten Visp)*

D. Fellner

*AXPO Hydraulic Energy Division (formerly NOK), Baden, Switzerland*

**ABSTRACT:** In the Glarner Alpes, about 90 km south-east of Zurich (Switzerland), construction has begun at an altitude of 2,400 m above sea level on a 1,000 MW hydro-power plant. The machine and the transformer cavern are situated in Quintner limestone under 400-500 m overburden. After the initial project design, their location had to be moved in accordance with the findings of additional geological investigations. Sensitivity analyses of rock mass parameters indicate also that the planned rock bolting system needs to be adapted.

## 1 INTRODUCTION

### 1.1 Purpose of the pumped storage scheme

The demand for sustainable power generation together with the accelerated retreat of glaciers and the predicted change of rainfall regimes urges Switzerland to economize its water resources. Underground pumped-storage plants supply valuable peak electricity while minimizing the impact on the natural heritage and the water consumption.

The power stations belonging to the Linth Limmern AG (KLL) in Glarus were built between 1957 and 1968. From a catchment area of 140 km<sup>2</sup> they produce about 460 kWh per annum. By virtue of their pumping capability, however, their significance in providing peak-load energy across Switzerland is much greater.

The project Linthal 2015 upgrades the KLL with an additional high-capacity pumped storage plant. A new underground facility will pump water from lake



Figure 1. Situation of the plant between the lower reservoir lake Limmern and the upper reservoir lake Mutt.

Limmern 630 m back up to lake Mutt. This will boost KLL's output from the current 450 kWh to 1,450 kWh, a performance on par with the Leibstadt nuclear power plant or the Cleuson Dixence hydro-power scheme.

### 1.2 Plant layout and structural design

A gravity dam will be built at lake Mutt to raise its current natural level of 2,446 m to 2.474 m a.s.l., thereby increasing its storage capacity from 9 to 25 million m<sup>3</sup>. The new Limmern power station will be installed about 600 m inside the mountain at approx. 1,700 m a.s.l. at the foot of lake Limmern (Fig 1).

Access to the underground caverns will be provided by cable car trough a 4 km long tunnel from Tierfehd, where an additional compensating basin is presently built to enable the machines to be used more flexibly for turbinning or pumping and to improve the regulation of flow in the river Linth.

As is common for large underground powerhouses, the four pumping-turbines are accommodated in a machine cavern, separated from the transformer cavern above the tailrace galleries (Fig 2).

The machine cavern has a length of 149 m, a width of 39 m and a height of 52 m. The side walls are pitched inwards to obtain a better stress distribution in the rock. The shorter and smaller transformer cavern has vertical side walls.

A critical design element is the width of the rock pillar separating the two caverns, which is intersected not only by the tailrace galleries below, but also by several access and cable galleries. With view to geotechnical stability, a wider spacing of the caverns is desirable, while from the operational point of view a shorter distance is to be preferred.

The distance adopted from preliminary elastic design (EXAMINE-2D) was 61 m between axes, resulting in 39 m width of the central pillar.

## 2 GEOLOGY

### 2.1 Initial data

According to prior knowledge and data gathered in 2007, the two main caverns were expected to become situated in predominantly massive limestones of the Quintner formation:

Table 1. Estimated rock mass properties (2008)

internal angle of friction $\phi$	39 ± 3	°
cohesion $c$	8 ± 4	MPa
uniaxial compressive strength $\sigma_{ci}$	90 ± 20	MPa
Young's modulus $E$	26 ± 4	GPa
deformation modulus $V$	20 ± 5	GPa
global strength index $GSI$	75 ± 5	-

The lower values represent residual properties ("parameter set B"). However, the primary set of parameters (called "A") was derived from a pessimistic estimate of  $GSI = 65$  together with  $\sigma_{ci} = 70$  MPa through a Hoek-Brown material model (ROCLAB), which gave for 520 m depth equivalent Mohr-Coulomb parameters of  $\phi = 38.3^\circ$  and  $c = 2.5$  MPa.

### 2.2 Exploration of geotectonical characteristics

In 2007 a horizontal exploration gallery was driven through the planned position of the main caverns. In several side galleries the orientation and persistence of discontinuities was registered along three scan lines of 10-15 m length each and in several borehole scans. However, the orientation of a primary joint set  $K_1$  and secondary joint sets  $K_2$  to  $K_4$ , accompanied by a schistose set  $S_0/S_S$ , varied between scan lines and borehole scans.

Table 2. Estimated joint properties

angle of friction in joints $\phi$	33 ± 3	°
cohesion $c$ on $K_1$	0.15 ± 0.1	MPa
cohesion $c$ on $K_2$ an $S_0/S_S$	2 - 4	MPa

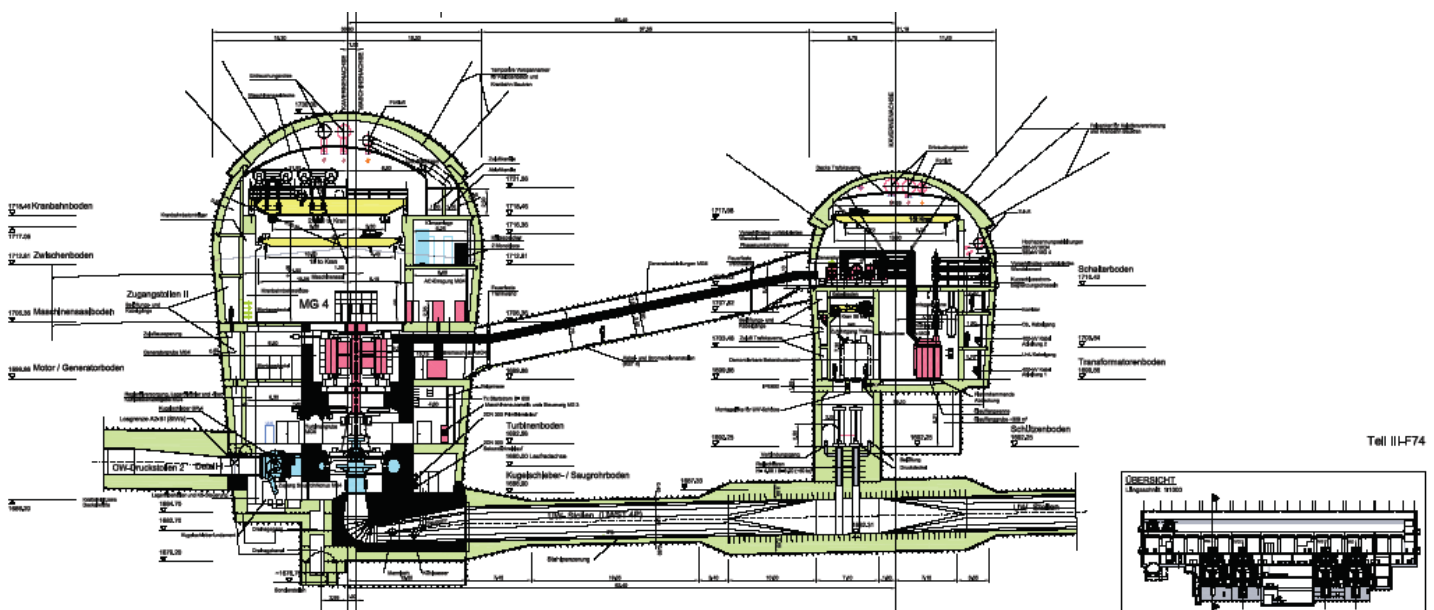


Figure 2. Cross-section of main caverns (basic design with 39 m clear distance between caverns).

Based on the findings from surface mapping, boreholes and exploration galleries, the main caverns were oriented perpendicular to the joint set  $K_1$ . During exploration a discrete fault zone and a fault related open karst pipe were found to intersect the rear end of the machine cavern, which prompted a relocation of the power-house ensemble away from the karst and fault and closer to the Linth valley.

### 2.3 Assumed in-situ stress regime

The topology above the caverns is characterized by the slope from the upper to the lower reservoir and a steep rising mountain flank parallel to the lake Limmern. This steep sloping suggested elevated lateral pressures both perpendicular and longitudinal to the cavern axes, except near the karst feature due to stress relief. It was thus concluded to vary the horizontal primary stresses between 0.28 and 0.70 of the vertical overburden pressure.

## 3 ANALYSES OF THE BASIC DESIGN

### 3.1 Hazard scenarios

During excavation of the caverns two principal hazards were considered important – the falling of key blocks from the crown, and the formation of wide failure zones in the walls. Other scenarios, such as an unfavourably inclined discontinuity bisecting the central pillar or the squeezing-in of a block at the cavern wall were disregarded on the grounds of the joint pattern and low joint persistence predicted.

Potentially mobile key blocks in the crown require deep prestressed rock bolting reaching behind discontinuities in order to avoid loosening. Moreover, the design includes a concrete arch supporting the crown before excavation of the benches.

In the final state, after the interior linings, including slabs, have been erected, all of the rock bolts and shotcrete are presumed to deteriorate and become ineffective. Thus in the long term, all rock loads must be carried by the permanent concrete lining.

### 3.2 Computational models

Discontinuum and continuum aspects were treated in separate models. The size and mobility of key blocks was assessed in 3D with the software UNWEDGE (Fig. 3). The extension of failure zones was studied for various combinations of rock properties and lateral pressure coefficients in a 2D plane strain model with the FEM software Z\_SOIL.PC (Figs. 4 & 5). The sensitivity to boundary conditions and angle of dilatancy was also investigated.

The three-dimensional geometrical effects were included by checking the influence of stress concentrations at the corners with “local” 3D meshes with approximate planes of symmetry.

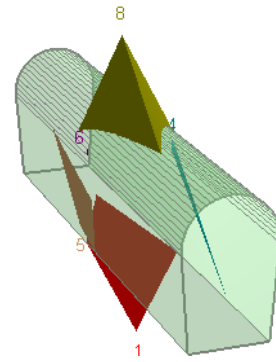


Figure 3: Analysis of key blocks for the machine cavern.

### 3.3 Results at the time of basic design

The dominating influence of the cohesion became apparent by the fact, that the “parameter set B” with  $c = 4$  MPa, despite a lower friction angle, yielded much smaller failure zones than “set A” with  $c = 2.5$  MPa. A higher primary horizontal stress level (0.70 instead of 0.50) produced 20% more wall displacement, although the size of failure zones decreased.

As can be seen from Figure 4, the rock bolts – considered as  $\varnothing 30$  mm at a pattern of  $1.7 \text{ m} \times 1.7 \text{ m}$  with 8 m length – act as “floating reinforcement” within the failure zones at the walls of the machine cavern. The vertical stress in the pillar reaches 25 MPa near the transformer cavern, which amounts to twice the primary stress.

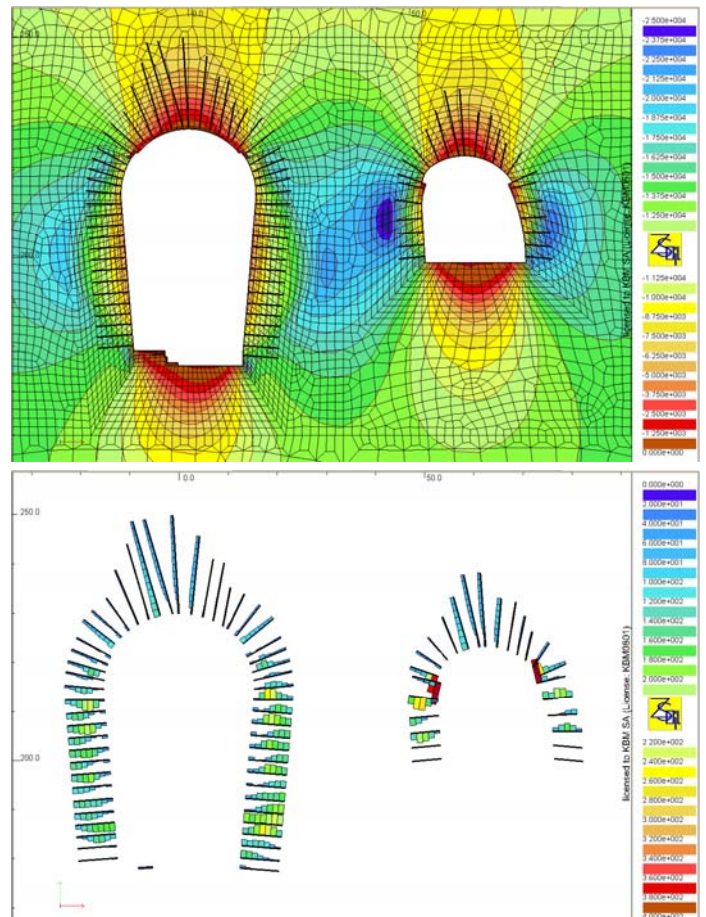


Figure 4. Vertical stresses and anchor forces for “set A” with  $K_0 \text{ lateral} / K_0 \text{ longitudinal} = 0.50 / 0.28$ ; clear cavern distance 39 m.

A successive  $c$ - $\tan\phi$ -reduction gave a factor of only 1.15 against complete plasticizing of the central pillar, increasing the displacement of the right-hand wall of the machine cavern from 3.0 to 4.8 cm.

## 4 ANALYSES OF THE REVISED DESIGN

### 4.1 Rock mass parameters

Laboratory and dilatometer tests revealed that the Quintner limestone might exhibit in fact a higher elastic modulus but considerably lower compressive strength. Moreover, a more platy and schistose zone was found to partly intersect both caverns (Tab. 2).

Table 2. Revised rock mass properties (2009).

massive-blocky limestone:		
internal angle of friction $\phi$	$43 \pm 3$	$^{\circ}$
cohesion $c$	$4 \pm 2$	MPa
uniaxial compressive strength $\sigma_{ci}$	$70 \pm 10$	MPa
Young's modulus $E$	$35 \pm 10$	GPa
deformation modulus $V$	$20 \pm 5$	GPa
global strength index $GSI$	$75 \pm 10$	-
platy-schistose limestone (mean values $\perp$ and $\parallel$ ):		
internal angle of friction $\phi$	$37 \pm 3$	$^{\circ}$
cohesion $c$	$1.5 \pm 0.5$	MPa
uniaxial compressive strength $\sigma_{ci}$	$50 \pm 10$	MPa
Young's modulus $E$	$20 \pm 5$	GPa
deformation modulus $V$	$10 \pm 5$	GPa
global strength index $GSI$	$50 \pm 10$	-

From comparison with the Hoek-Brown failure criterion, the values of Table 3 were agreed for the purpose of analysis, including a drop from peak to residual strength (cf. Cai et al. 2007).

Table 3. Agreed peak and residual strength (2009).

massive-blocky limestone:		
	peak	residual
uniaxial compressive strength $\sigma_{ci}$	80 MPa	
global strength index $GSI$	70	45
internal angle of friction $\phi$	$47^{\circ}$	$40^{\circ}$
cohesion $c$	3.0 MPa	1.5 MPa
platy-schistose limestone (mean):		
	peak	residual
uniaxial compressive strength $\sigma_{ci}$	50 MPa	
global strength index $GSI$	45	35
internal angle of friction $\phi$	$36^{\circ}$	$33^{\circ}$
cohesion $c$	1.3 MPa	1.0 MPa

### 4.2 Results

The influence of the revised geological model and rock mass parameters was explored in plane strain FEM with codes allowing for a brittle strength drop in Mohr-Coulomb material (PHASE<sup>2</sup>, PLAXIS).

For comparison, the elastic and strength anisotropy of the platy-schistose limestone was also modeled by means of a multi-laminate ("jointed rock") constitutive law. However, the variation of the dipping angle that had to be included led to unrealistic local failure. It was thus decided to treat the platy limestone as isotropic with mean parameters.

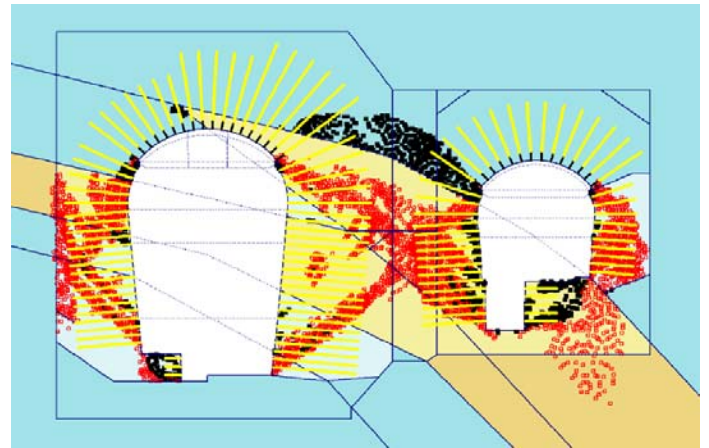


Figure 5. Failure zone with bands of platy limestone and 16 m long rock bolts for 39 m clear cavern distance ( $K_0 = 0.40$ , isotropic drop to residual strength in PLAXIS).

### 4.3 Conclusion

The revised analysis revealed that the failure zones of both caverns overlap for a 39 m wide pillar even when the rock bolt pattern is intensified and the length of bolts increased to 16 m (Fig. 5). Therefore other distances between caverns were investigated, resulting in reduced wall displacements (Tab. 4).

Table 4: Displacements of the right wall of the machine cavern for different failure criteria (deformation moduli  $V = 25$  GPa, resp. 12 GPa in the weak zone).

clear cavern distance	39 m	59 m
weak zone isotropic (peak strength)	3.9 cm	2.3 cm
weak zone isotropic (drop to residual)	6.7 cm	3.7 cm
weak zone as jointed rock	4.0 cm	2.7 cm

By adopting the philosophy that the excavation of the transformer cavern should not increase the wall displacements of the prior constructed machine cavern by more than 10%, it was decided to enlarge the clear spacing of caverns to 59 m.

## 5 ANALYSIS FOR FINAL DESIGN

Further 2D FEM analyses are planned of two different sections using the Hoek-Brown failure criterion with softening to optimize the pattern and length of rock bolts which are to be prestressed. To account for the intersecting galleries, additional 3D computations may be carried out with Z\_SOIL.PC, employing Menétrey's generalization (1994) of the Willam failure criterion for damage in triaxial compression.

## REFERENCES

- Cai, M. et al. 2007, Determination of residual strength parameters of jointed rock masses using the GSI system. *Int. J. Rock Mechanics & Mining Sciences* 44, 247-265.
- Menétrey, Ph. 1994, *Numerical analysis of punching failure in reinforced concrete structures*. PhD Thesis, EPF Lausanne.